Biochimica et Biophysica Acta 1830 (2013) 4554–4563

Contents lists available at SciVerse ScienceDirect

Biochimica et Biophysica Acta

journal homepage: www.elsevier.com/locate/bbagen

Kinetic uptake profiles of cell penetrating peptides in lymphocytes and monocytes

Margarida Rodrigues [a], Beatriz G. de la Torre [b], David Andreu [b,*], Nuno C. Santos [a,**]

[a] Instituto de Medicina Molecular, Faculdade de Medicina, Universidade de Lisboa, Lisbon, Portugal
[b] Department of Experimental and Health Sciences, Pompeu Fabra University, Barcelona Biomedical Research Park, Barcelona, Spain

ARTICLE INFO

Article history:
Received 3 January 2013
Received in revised form 7 May 2013
Accepted 14 May 2013
Available online 24 May 2013

Keywords:
Nucleolar targeting peptide
Cell penetrating peptide
Lymphocyte
Monocyte
Uptake
Kinetics

ABSTRACT

Background: Nucleolar targeting peptides (NrTPs), resulting from structural minimization of the rattlesnake toxin crotamine, are a novel family of cell-penetrating peptides (CPPs) shown to internalize and deliver cargos into different cell types.
Methods: In this study, we address NrTP kinetics of translocation into primary cells. We used flow cytometry to measure the intracellular uptake of rhodamine B-labeled NrTPs in peripheral blood mononucleated cells (PBMCs).
Results: The kinetic profiles for each peptide are concentration-independent but significantly different among NrTPs, pointing out for the amino acid sequence importance. Arginine-containing peptides (NrTP7 and $Tat_{48–60}$, used for comparison) were found to be more toxic than lysine-containing ones, as expected. On the other hand, one same peptide behaves differently in each of the lymphocyte and monocyte cell populations, suggesting differences in entry mechanism that in turn reflect diversity in cell functionality. Uptake results obtained at 4 °C or using chemical endocytosis inhibitors support the importance of non-endocytic mechanisms in the cellular internalization of NrTP1 and NrTP5, while confirming endocytosis as the main mechanism of NrTPs entry.
Conclusion: Overall, both direct translocation and endocytosis mechanisms play a role in NrTP entry. Yet, there is predominance of endocytosis-mediated mechanisms. NrTPs (especially NrTP6) are an excellent intracellular delivery tool, with efficient internalization and no toxicity.
General significance: This work validates NrTPs as potential therapeutic tools for, e.g., cancer or inhibition of viral replication and establishes a new comparative and quantitative method to test CPP efficiency.

1. Introduction

Cell-penetrating peptides (CPPs) are receiving increasing attention as an innovative concept in therapeutics, for their role as delivery shuttles. They are able to deliver different molecular cargos (e.g., imaging agents, drugs, proteins, plasmid DNA, siRNA, nanoparticles or bacteriophages) both in vitro and in vivo [1,2]. The use of CPPs as drug carriers may overcome limitations such as poor drug bioavailability, low clinical efficacy [3], or undesirable side-effects. There is significant interest on these peptides in areas of application such as skin diseases (CPPs for topical application), myocardial infarction, ischemia, pain, splicing correction, HIV vaccines and several different cancers [4–6]. The first CPP-based drug reached phase II clinical trials in 2003 and, from then on, the number of peptides under trial has not stopped increasing [7,8].

Despite the widespread interest in CPPs, the mechanisms underlying their cellular translocation are poorly understood and subject to discussion. It is generally believed that there is not a universal translocation mechanism for all CPPs; instead, some use endocytosis-mediated mechanisms, others direct translocation by energy-independent mechanisms, while others may use both [9]. HIV-derived CPP $Tat_{48–60}$ is proposed to enter via direct translocation [10], while penetratin ($pAntp_{43–58}$), another well-studied CPP, was shown to use both endocytosis and direct translocation [9]. Other factors influencing CPP entry mechanisms are the nature and size of the cargo, as well as the type of target cell or tissue [11]. For example, when conjugated to large molecules Tat internalizes by endocytosis-mediated mechanisms [12].

The CPPs in this work belong to the family of nucleolar targeting peptides (NrTPs), designed by structural minimization of crotamine, a main component of the venom from the South-American rattlesnake *Crotalus durissus terrificus*. NrTPs were first reported in 2008 as capable of entering HeLa cells and localizing in their nucleolus [13]. The potential of NrTPs to interact with membranes was assessed in studies with lipid model systems [14], and their ability to deliver large cargos in native

Abbreviations: Ahx, 6-aminohexanoic acid; AMP, antimicrobial peptide; CPPs, cell penetrating peptides; HPLC, high-performance liquid chromatography; NrTPs, nucleolar-targeting peptides; PBMCs, peripheral blood mononucleated cells; RhB, rhodamine B; CPZ, chlorpromazine; FITC, fluorescein isothiocyanate; FSC, forward scatter; SSC, side scatter

* Correspondence to: D. Andreu, Department of Experimental and Health Sciences, Pompeu Fabra University, Barcelona Biomedical Research Park, Dr Aiguader 88, 08003 Barcelona, Spain. Tel.: +34 933160868; fax: +34 933160901.
** Correspondence to: N.C. Santos, Instituto de Medicina Molecular, Faculdade de Medicina, Universidade de Lisboa, Av. Prof. Egas Moniz, 1649-028 Lisbon, Portugal. Tel.: +351 217999480; fax: +351 217999477.
E-mail addresses: david.andreu@upf.edu (D. Andreu), nsantos@fm.ul.pt (N.C. Santos).

0304-4165/$ – see front matter © 2013 Elsevier B.V. All rights reserved.
http://dx.doi.org/10.1016/j.bbagen.2013.05.020

form was demonstrated with β-galactosidase, a 465 kDa tetrameric protein that retained enzymatic activity after both NrTP conjugation and cell internalization [15]. More recently, further insights into the uptake mechanism have been obtained from both confocal microscopy and flow cytometry studies [16].

In the present work, in order to further explore the potential of NrTPs as in vivo delivery agents, we have used human primary immune cells, specifically fresh peripheral blood mononuclear cells (PBMCs), as a model. PBMCs can be divided into two main populations: lymphocytes and monocytes, both involved in fighting infection and adapting to intruders, yet with completely different functions in the organism. Different subsets of lymphocytes perform a variety of functions within the immune system: helper T cells regulate other immune cells; cytotoxic T and NK cells lyse virus-infected cells, tumor cells and allografts; B cells secrete antibodies. Monocytes, for their part, are involved in phagocytosis, antigen presentation and cytokine production, and are the precursors of macrophages and dendritic cells [17]. PBMCs can either be directly involved in pathologies such as leukemia and HIV-1 infection, or play an important role in virtually any pathology, as part of the immune system. Studying PBMCs in terms of CPP uptake efficiency may help find applications for CPPs in immunology. To this end, we have developed an efficient method to detect and quantitatively compare differences in PBMC uptake among NrTPs that may reveal details of their translocation mechanism. Furthermore, we have studied the effect of amino acid residue substitutions in NrTP uptake efficiency and toxicity.

2. Material and methods

2.1. Materials

Ficoll-Paque Plus was from GE Healthcare. TO-PRO3, Hoechst 33342 and trypan blue were from Invitrogen. Annexin V-FITC conjugate was from BD Pharmingen, while dynasore and chlorpromazine were from Sigma.

2.2. Peptides

The solid phase synthesis of N-terminal rhodamine B (RhB)-labeled peptides NrTP1 (YKQCHKKGGKKGSG), NrTP2 (with a 6-aminohexanoic acid spacer between GG and KK), NrTP5 (enantiomer of NrTP1), NrTP6 (Cys residue replaced by Ser), NrTP7 (all 5 Lys residues changed to Arg) and NrTP8 (Tyr replaced by Trp) have been described earlier [13,18]. $Tat_{48–60}$ (GRKKRRQRRRPPQ-amide) was similarly synthesized by solid phase methods. All peptides were purified to >95% homogeneity by analytical HPLC and had the expected molecular masses. Sequences are shown in Table 1.

2.3. Isolation of PBMCs

Human blood samples were collected from healthy blood donors, with their previous written informed consent, following a protocol established with the Portuguese Blood Institute (Lisbon), approved by the Ethics Committee of the Faculty of Medicine of the University of Lisbon. Human PBMCs were isolated by density gradient using Ficoll-Paque Plus (GE Healthcare, Little Chalfont, UK). Briefly, the collected blood sample is diluted 1:1 (v/v) with PBS, pH 7.4, and carefully added to Ficoll-Paque, 1:0.6 (v/v), in order to avoid mixing. After centrifugation at 400 *g* for 40 min at 18–20 °C, the cloudy interphase between plasma and Ficoll-erythrocytes corresponds to the PBMCs layer. These cells are gently aspirated, washed with PBS and centrifuged at 100 *g* for 10 min. This step is repeated three times. In the last repeat, cells are resuspended in PBS supplemented with 2% fetal bovine serum (FBS). All reagents were used at room temperature. Experiments started immediately after PBMC isolation.

Table 1
NrTPs and reference CPP used in this study.

Peptide	Sequence[a]	Comments
NrTP1	YKQCHKKGGKKGSG	Derived from crotamine by N- to C-terminal
NrTP2	YKQCHKKGG-Ahx-KKGSG	endpiece splice, with or without Ahx spacer [13]
NrTP5	ykqchkkGGkkGsG	Enantiomer of NrTP1
NrTP6	YKQSHKKGGKKGSG	Cys in NrTP1 replaced by Ser
NrTP7	YRQSHRRGGRRGSG	All Lys in NrTP6 replaced by Arg
NrTP8	WKQSHKKGGKKGSG	Tyr in NrTP6 replaced by Trp
$Tat_{48–60}$	GRKKRRQRRRPPQ	broadly used CPP [10]

[a] Lower case letters denote D-amino acid residues. All sequences were labeled with rhodamine B (RhB) at the N-terminus.

2.4. Flow cytometry

Experiments were done in a BD FACSAria III, using a yellow-green (561 nm) laser to excite rhodamine B, which was detected using a 582/15 filter. 10,000 events were recorded on each measurement. Briefly, PBMCs suspensions were prepared at 2×10^6 cells/mL. Each peptide was added to the corresponding tube immediately after the $t = 0$ min reading. Peptide concentrations used in the kinetic assays were 2, 5 and 15 μM and measurements were made every 10 min. The cells were kept at 37 °C in a thermostatized bath during the entire experiment (2 h) as well as on the detection chamber of the cytometer. Tubes were gently flickered before and after the reading to ensure proper cell homogeneity. At least one control tube of unstained cells was tested per day of experiment. Each concentration of each peptide was tested at least three times. Peptide uptake at 4 °C was also followed for 2 h, with readings every 10 min, as described above.

Dose–response experiments were performed as end point measurements, with readings after 2 h incubation with peptide concentrations ranging from 1 to 20 μM at 37 °C. Measurements with endocytosis inhibitors were also done after 2 h incubation with 5 μM peptide. Chlorpromazine (CPZ) (5 or 50 μM) or dynasore (80 μM) were added to cells 30 min prior to peptide [16,19,20]. Dynasore assays were carried out in the absence of serum [19]. Specific controls were carried out for each independent experiment: cells only, and cells with CPZ (5 or 50 μM), dynasore (80 μM) or DMSO 2% (v/v; dynasore vehicle).

Following 2 h incubation with NrTPs and the corresponding reading, TO-PRO3 (viability dye) was added to the cell suspension to a final concentration of 0.25 μM [18]. After 10 min incubation with the probe, a new measurement was taken using the red (640 nm) laser to excite and the emission filter 670/14 to detect TO-PRO3 fluorescence. The influence of NrTPs on the viability of PBMCs was further studied using annexin V. Samples resulting from the 2 h incubation of 15 μM NrTPs with PBMCs were centrifuged at 150 *g* for 5 min in an Eppendorf miniSpin centrifuge. Supernatant was discarded and cells were resuspended in 100 μL of buffer with 0.1% annexin V and left to stain in the dark, for 15 min, at room temperature. Prior to analysis, samples were further diluted with 100 μL of annexin V buffer. Samples were measured in the same flow cytometer, using a blue (488 nm) laser to excite and a 530/30 filter to detect FITC fluorescence. All flow cytometer results were analyzed using FlowJo Software version 9. Events were gated to the population of lymphocytes and monocytes according to their forward scatter (FSC) and side scatter (SSC). Curve fitting and statistical analysis were done using GraphPad Prism.

2.5. Live cell microscopy

Microscopy experiments were carried out in a Zeiss LSM 510 META confocal point-scanning microscope (Jena, Germany). Diode 405–30 (405 nm; 50 mW), diode-pumped solid-state (DPSS; 561 nm; 15 mW) and HeNe633 (633 nm; 5 mW) lasers were used with a 63× oil-objective of 1.4 numerical aperture. Cells were incubated with NrTPs for 2 h prior to imaging. They were labeled with Hoechst (nuclear

stain) 2.5 μg/mL for 20 to 30 min and with TO-PRO3 (viability) 0.25 μM for 10 to 15 min, before imaging. The cell suspension (200 μL) was deposited in 8-well Ibidi-treated plates (μ-slide 8 well; Ibidi, Munich, Germany). Images were processed using Zeiss software and ImageJ (rsbweb.nih.gov/ij/).

3. Results

3.1. Internalization of NrTPs into PBMCs

Table 1 shows the sequences of the six NrTPs used in this study. NrTP1 and NrTP2 are directly derived from crotamine by N- to C-terminal end piece splicing, with or without the 6-aminohexanoic acid spacer, respectively. Although the risk of dimerization of the Cys residue in NrTP1 was found to be non-significant [13], in NrTP6 and subsequent analogs Cys was replaced by Ser for extra precaution. The other replacements on NrTP7 and NrTP8 are typical in peptide structure–activity studies. Thus, in NrTP7 all Lys residues were replaced by Arg, a more basic amino acid, known to enhance CPP activity [21]. For NrTP8, Tyr was replaced by Trp, a better fluorophore. All these variations may influence uptake and provide insights on the internalization mechanism.

Fig. 1 shows a representative confocal image of NrTP6 localization in PBMCs, after 2 h incubation at 37 °C. All other peptides in the study were also able to translocate into primary PBMCs. While no significant variations in localization were observed, some changes in fluorescence intensity and distribution reflected differences in internalization, as discussed below. Although NrTPs exhibit strong nucleolar labeling in some cell types [13], in PBMCs the peptide stays mostly in the cytosol.

3.2. Kinetic profile of NrTPs uptake

To compare the kinetics and extent of uptake in PBMCs, the increase in fluorescence for all NrTPs and $Tat_{48–60}$ was monitored by flow cytometry over 2 h at 10 min intervals. PBMCs were gated according to the FSC and SSC values, for lymphocyte and monocyte populations (Fig. 2A). Fig. 2B shows representative histograms of RhB fluorescence time courses. In the absence of peptide, fluorescence was negligible; hence RhB intensity was adopted as a measure of PBMC-internalized peptide. This assumption relies on two important observations: (1) by confocal microscopy the peptide is found to accumulate in the cytoplasm rather than on the cell membrane; (2) cytometry fluorescence readings were unaffected by the presence of trypan blue (a membrane-impermeable RhB quencher) [22,23].

Fig. 3 shows uptake kinetic profiles for all NrTPs and the $Tat_{48–60}$ control at 2, 5 or 15 μM concentration, for both lymphocytes and monocytes. The fluorescence intensity scale (*yy* axis) was set to be proportional to the respective peptide concentration. This choice was done in order to facilitate comparisons between the different concentrations used for all peptides tested. The plots show that fluorescence intensity depends on initial peptide concentration. In lymphocytes, an approximately linear dependency can be observed, with uptake following the general trend $Tat_{48–60}$ < NrTP1 < NrTP5 < NrTP8 < NrTP2 < NrTP7 < NrTP6. For monocytes, a ranking was harder to establish because, for some peptides, uptake varied significantly with concentration (e.g., NrTP2 and NrTP7 had rather different uptakes at low concentration, but at 15 μM gave similar fluorescence values). Other observed differences of monocytes relative to lymphocytes were: the linear behavior of NrTP5 at all concentrations tested; the drop in fluorescence for NrTP7 at 5 and 15 μM, after reaching a maximum intensity (probably reflecting a mild toxicity effect); and also the highest uptake of NrTP2 in monocytes, in contrast to lymphocytes, where it behaves very similarly to NrTP1.

Fig. 4A–B, displaying NrTP1 uptake curves for both cell populations at three concentrations and normalized to the maximum intensity, shows that the kinetic profile is not concentration-dependent. The same is observed for the other NrTPs (see Supplementary information Fig. S1). Fig. 4C–D shows normalized uptake profiles, for both cell populations, of all six NrTPs at 15 μM (for 2 and 5 μM profiles see Supplementary Information Fig. S2). As profiles are plotted for the same concentration, differences in the time taken for each peptide to reach its equilibrium plateau (resulting from the entry rate) are significant. A first observation in this regard is the significant variation observed between populations, entry rates being higher for lymphocytes than for monocytes. Also, differences among individual peptides appear more significant in lymphocytes than in monocytes (except for NrTP5). In lymphocytes, NrTP1, NrTP2, NrTP5 and NrTP8 have faster kinetics, while NrT6, NrTP7 and $Tat_{48–60}$ have slower ones. To facilitate comparison, quantitative analysis using a saturation empirical model was found to fit well most of the data, yielding the useful parameters defined in Eq. (1):

$$I = \frac{I_{max} \times t^h}{t_{1/2}^h + t^h} \quad (1)$$

where I_{max} is the maximum value for the fluorescence intensity (proportional to the amount of internalized peptide), $t_{½}$ is the half-time needed to reach I_{max}, and h is the Hill slope, used to

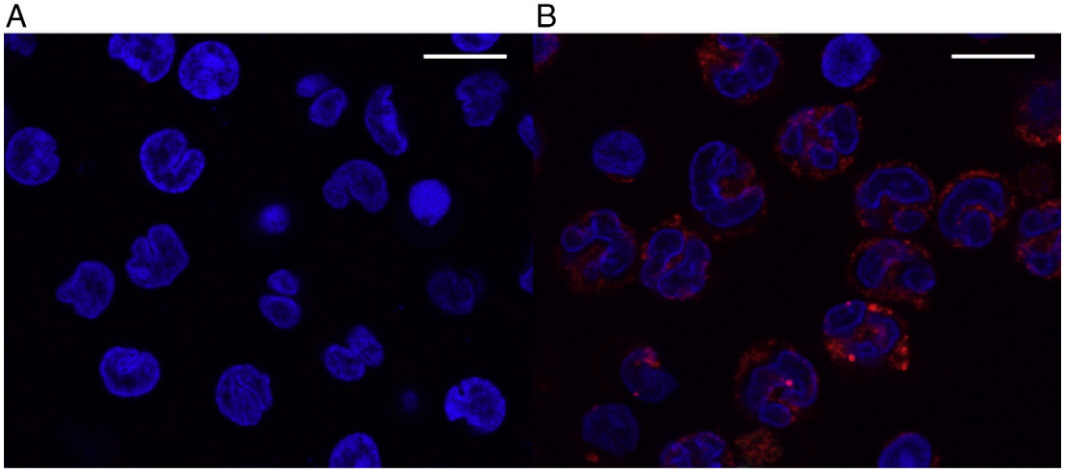

Fig. 1. PBMCs incubated with NrTP6. Confocal microscopy images for PBMCs in the absence (A) and after 2 h incubation with RhB-labeled NrTP6 15 μM (B), at 37 °C. RhB (red) and Hoechst (blue) are detected upon excitation with 561 nm and 405 nm lasers, respectively. Scale bars = 10 μm.

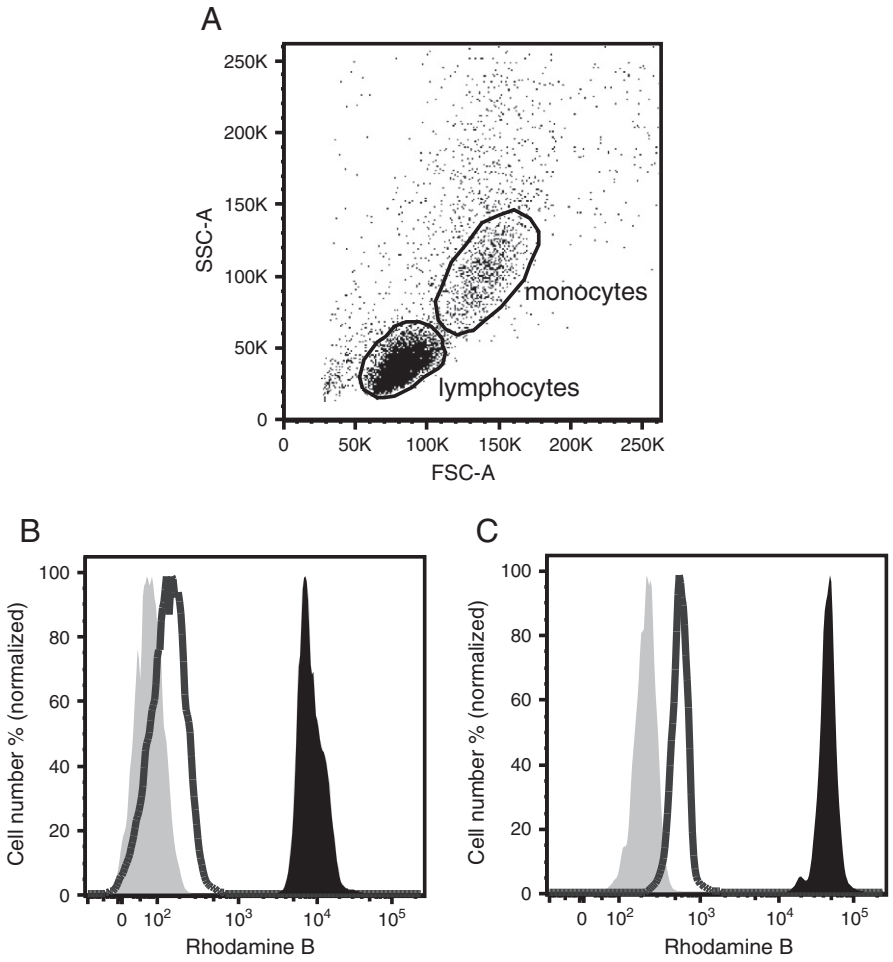

Fig. 2. Flow cytometry settings for the study of NrTP uptake by PBMCs. Gates for lymphocytes and monocytes were set according to cell distribution in FSC vs. SSC dotplot (A). Representative fluorescence intensity histograms for lymphocytes (B) and monocytes (C); depicted are the changes with time in the fluorescence of cells unstained at 0 (filled in gray) and 2 h (line), and after 2 h incubation with NrTP6 (filled in black).

characterize the initial curve behavior that gives the profile a sigmoid shape. When this sigmoid behavior is absent, h equals 1 and Eq. (2), used earlier in CPP kinetic analysis [24], is obtained:

$$I = \frac{I_{max} \times t}{t_{1/2} + t}. \quad (2)$$

Whereas lymphocyte results could be properly fitted to the simpler Eq. (2), monocyte data required an $h \neq 1$ for the fitting. Results from data fitting at 15 μM are shown in Table 2 (for other concentrations see Supplementary Information). For each PBMC population, values were normalized to the highest value of I_{max} or $t_{½}$. As previously mentioned, NrTP6 exhibited the highest level of internalization in lymphocytes, followed by NrTP7. $Tat_{48–60}$, despite its $t_{½}$ closer to NrTP6 and NrTP7, was the least internalized peptide. NrTP1, NrTP2, NrTP5 and NrTP8 had intermediate kinetics, faster than $Tat_{48–60}$, with $t_{½}$ around 10 min. In monocytes, NrTP6 and NrTP7 again displayed the highest uptake rates, although I_{max} differences among peptides were less pronounced than for lymphocytes. NrTP5 results could not be fitted to the model, due to its linear tendency during the 2 h of experiment.

Further on, longer incubation times, up to 24 h, were also explored (see Supplementary Information Fig. S6). The only significant changes occurred for NrTP5 and NrTP7. NrTP5 fluorescence increased from 2 to 24 h for all concentrations tested. As this peptide had an approximately linear kinetic profile for the first 2 h, a further increase in fluorescence was expectable, suggesting a slower uptake for NrTP5 than for the rest of peptides. In contrast, for NrTP7 fluorescence decreased, especially in lymphocytes, from 2 to 24 h incubation, a finding also anticipated by the decrease tendency of its kinetic profiles.

3.3. Cell viability tests

The potential of CPPs as delivery agents largely depends on their lack of toxicity. To evaluate cell viability in NrTPs, variation in cell number was monitored for each cell population over 2 h NrTP exposure. Fig. 5A–B shows that NrTP-caused cell death was negligible in PBMCs. In lymphocytes, only NrTP7 and $Tat_{48–60}$, caused substantial levels of cell loss (50% and 30%, respectively) at 15 μM. In monocytes, cell numbers varied significantly only for $Tat_{48–60}$ at 15 μM.

While cell number variation is a good readout of NrTPs toxicity, we also found it important to assess the viability of the remaining cells after 2 h. For that purpose, TO-PRO3 and annexin V were used as viability probes. TO-PRO3 is a membrane-impermeable dye that binds strongly to dsDNA only when membrane integrity is compromised. Its far-red fluorescence (642–661 nm) and almost no spectral overlap with green and red fluorophores make TO-PRO3 an excellent alternative to propidium iodide [18], especially in three-color flow cytometry studies [25] like the present one, where NrTPs are RhB-labeled and annexin V is conjugated to FITC. Nevertheless, as TO-PRO3 may eventually penetrate live cells via P2x1-9 receptors or apoptotic cells, careful data interpretation is necessary. The percentage of cells internalizing TO-PRO3 was determined using the fluorescence intensity of ~90–95% of cells not exposed to any CPP as basal level. Results in Fig. 5B–C are

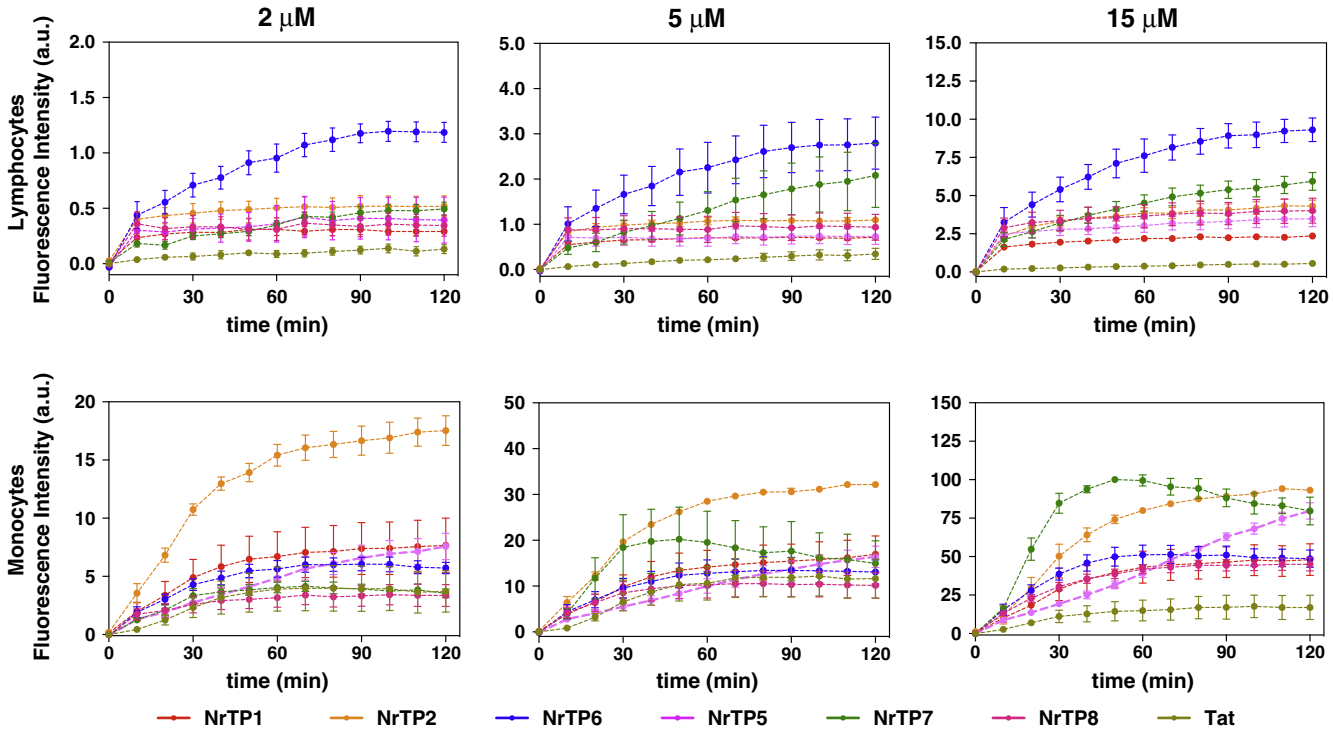

Fig. 3. Kinetic profiles for NrTPs and Tat_{48-60}. Each plot contains the profiles for all peptides tested for a given concentration (2, 5 or 15 μM), both in lymphocytes and monocytes. Error bars represent standard error (SEM) of 3 independent experiments.

in agreement with those obtained from variations in cell number. Thus, in lymphocytes, the percentage of cells that incorporate TO-PRO3 at 2 or 5 μM of peptide is not statistically different from control, except again for Tat_{48-60}. At 15 μM concentration of all peptides except NrTP1 and NrTP6, TO-PRO3 is able to penetrate cells. Nevertheless, it should be noted that these settings were established to maximize the differences

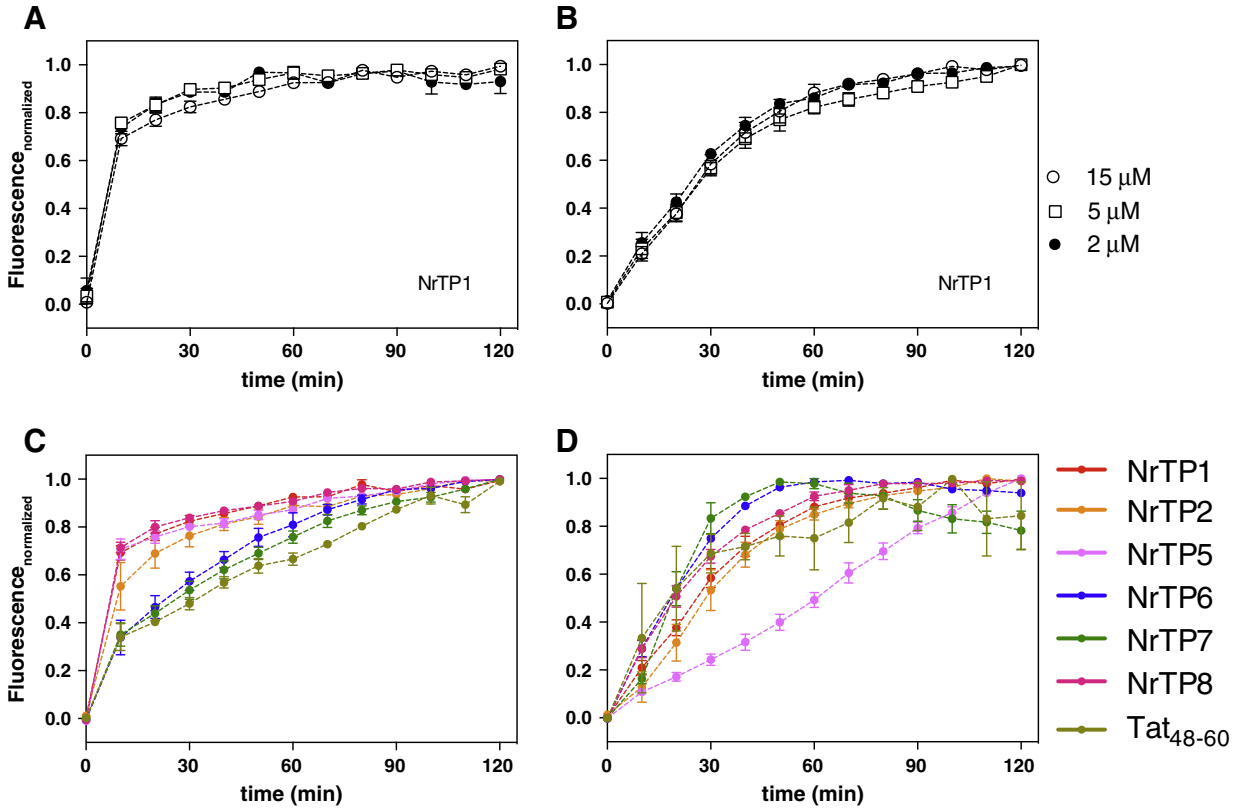

Fig. 4. Kinetic profiles normalized to the maximum fluorescence in lymphocytes (A and C) and monocytes (B and D). Normalized plots for NrTP1 (A and B) at 2 (●), 5 (□) and 15 (○) μM. Normalized plots for all peptides at 15 μM (C and D). Error bars represent SEM of at least 3 independent experiments.

Table 2
Results obtained by the fitting of the kinetic profiles for the peptides at 15 μM (using Eq. (1) for monocytes and Eq. (2) for lymphocytes): I_{max} (maximum intensity of rhodamine B fluorescence), $t_{1/2}$ (time to reach half of the maximum intensity), and $I_{max\ (normalized)}$ (values normalized for the highest I_{max}).

Peptide	Lymphocytes			Monocytes			
	I_{max} (a.u.)	$I_{max\ (normalized)}$	$t_{1/2}$ (min)	I_{max} (a.u.)	$I_{max\ (normalized)}$	$t_{1/2}$ (min)	h
NrTP1	2.4	0.20	6	51.9	0.52	26	1.74
NrTP2	4.6	0.38	11	99.8	1.00	30	1.99
NrTP5	3.5	0.28	5		–	–	–
NrTP6	12.2	1.00	33	52.8	0.53	17	2.08
NrTP7	7.7	0.63	37	92.1	0.92	17	3.80
NrTP8	4.2	0.35	5	50.0	0.50	21	1.49
$Tat_{48–60}$	0.9	0.07	48	19.7	0.20	26	1.78

in toxicity among NrTPs. PBMCs treated with 0.1% (v/v) Triton X-100 revealed approximately 16-fold higher fluorescence signal than the NrTP with the highest intensity (see Supplementary information Fig. S3). NrTP2, NrTP5 and NrTP8, though not causing cell death (Fig. 6A–B), seem to interfere with the stability and integrity of the membrane. Fig. 6E illustrates the contrast in toxicity between $Tat_{48–60}$ and NrTP6, as well as the differences in localization of both peptides.

For annexin V, an overall pattern similar to that of TO-PRO3 was found (see Supplementary Information Figs. S4 and S5): NrTP7 and $Tat_{48–60}$ had the highest percentages of annexin V-positive cells and NrTP6 the lowest. Differences between peptides were not as marked as in the cell number variation and TO-PRO3 tests. This might be due to false positives arising from the entry mechanism. Direct CPP translocation may involve deformations in the membrane and the formation of multilamellar, particle-like structures at the site of entry [26,27]. This would cause inversions in the exposure of the membrane leaflets, and therefore exposure of phosphatidylserine (PS, probed by annexin V), even though cell integrity would not be compromised. Other exceptions for positive labeling with annexin V include reversible exposure of PS, and PS exposure during T-cell activation, both occurring without cell death [28].

3.4. Influence of temperature and endocytosis inhibitors on NrTP uptake

In order to evaluate the importance of endocytosis in cell entry, NrTP1, NrTP5, NrTP6 and NrTP7 uptake was monitored at 4 °C. Kinetic profiles were conducted for 2 h, with readings every 10 min, as in the experiments at 37 °C. The maximum intensity at 4 °C for each of these peptides at 5 μM is shown in Fig. 6A–B (for results at 2 and 15 μM see Supplementary Information Fig. S7 A–B). Results are plotted together with those obtained at 37 °C and using chemical endocytosis inhibitors. There are statistically significant differences ($p < 0.0001$; two-way ANOVA) between internalization at 37 °C and 4 °C, underlying the importance of endocytosis-mediated mechanisms for NrTP cellular internalization. In lymphocytes, these differences were more extensive for NrTP6 and NrTP7, whereas in monocytes all peptides tested, with the exception of NrTP5, underwent a strong decrease in internalization at 4 °C. These results were further supported by confocal microscopy experiments (data not shown).

The comparison between the normalized kinetics at 37 °C and 4 °C for NrTP1 (Fig. 6C–D) suggests differences on the entry mechanism of NrTPs into the two cell populations. While for lymphocytes the kinetic profiles for both temperatures are very similar, in monocytes there are marked differences in their shape. For this last cell population, 4 °C uptake takes place within the first 10 min, while at 37 °C it continues for considerably longer, though with a progressively slower rate (for the normalized kinetic profiles of other peptides see Supplementary information Fig. S7).

In order to complement the studies regarding the entry mechanism of NrTPs, peptide internalization assays were performed using chemical inhibitors of endocytosis (Fig. 6A–B). Chlorpromazine (CPZ) is a cationic amphiphilic drug that inhibits clathrin-coated pit formation by a reversible translocation of clathrin and its adapter proteins from the plasma membrane to intracellular vesicles [29,30]. Of two concentrations (5 and 50 μM) tested in other studies [16,19], only the former was feasible, as in our system 50 μM CPZ dramatically compromised cell viability (for cell number variation see Supplementary Information Fig. S8A–B). Dynasore, on the other hand, is a cell-permeable, reversible noncompetitive inhibitor of the GTPase activity of dynamin 1 and dynamin 2 [20] that blocks dynamin-dependent endocytosis by compromising scission of endocytic vesicles [19,31]. As several endocytosis mechanisms depend on the action of dynamin, dynasore has a broader impact than CPZ on endocytosis impairment [32]. In contrast with CPZ, dynasore did not interfere with cell viability at the experimental conditions of our study.

In lymphocytes, 5 μM CPZ did not inhibit NrTPs uptake, as shown by the similar fluorescence values found at 37 °C for all peptides, with or without CPZ. In monocytes, some differences were observed, namely for NrTP1 ($p = 0.0331$; Dunnett's post-test). Dynasore, for its part, had a more pronounced effect. Thus, lymphocytes incubated with dynasore at 37 °C behaved similar to those at 4 °C without dynasore, except for NrTP6, for which inhibition was less pronounced, though statistically significant ($p < 0.0001$; Dunnett's post-test). For monocytes, with the exception of NrTP7, two distinct sub-populations could be distinguished regarding peptide fluorescence signal (see Supplementary Information Fig. S9): one (~40% cells) displayed fluorescence values consistent with uptake inhibition, while the other one did not. In terms of internalization efficiency and viability, the experiments showed variation trends similar to those of the kinetic assays. Thus, NrTP6 is the peptide preferentially internalized by PBMCs, without interference in cell counts or viability, whereas NrTP7 behaves similar to NrTP1 and NrTP5, but with the drawback of being slightly toxic (especially for lymphocytes); it is the only peptide causing cell loss in the experiments with both CPZ and dynasore.

Together, the results of internalization at 4 °C and in the presence of endocytosis inhibitors suggest that: i) clathrin-dependent internalization does not play a major role, if any, in NrTP uptake, once to do so, CPZ and dynasore should have parallel effects, and ii) endocytosis is the predominant route for NrTP internalization, with a lower role in NrTP1 and NrTP5 uptake, especially in lymphocytes. Also, the dynasore results point towards a dynamin-dependent endocytosis mechanism. Dynamin has been proven to be implicated in several endocytic mechanisms, namely clathrin-dependent endocytosis, phagocytosis, IL2Rβ (interleukin-2 receptor subunit β) pathway and circular dorsal ruffles endocytosis, plus a few others (such as caveolae/caveolin 1-dependent endocytosis and macropinocytosis) for which evidence is less persuasive [32]. Even if the first two seem excluded in the present case, a wide range of mechanisms for NrTP uptake remain possible, although at this time our results do not allow a final conclusion on which one is involved.

3.5. Dose response curves for NrTPs uptake

Dose response curves for NrTP1, NrTP5, NrTP6 and NrTP7 uptake are presented in Fig. 7. Together with the kinetic (Figs. 3 and 4) and viability data (Fig. 5), the curves provide a reliable assessment of the minimum and maximal peptide concentrations that can be used (and detected) without compromising viability. Hence, it is possible to identify the most efficient and safe peptide to be internalized by each PBMC population. Fluorescence signal detection was possible for peptide concentration as low as 1 μM, not only due to the high sensitivity of the flow cytometer, but also to the effectiveness of NrTP internalization. Experimental data was fitted to a semi-logarithmic empirical model [33–35],

$$I = I_{min} + \frac{I_{max} - I_{min}}{1 + 10^{h(\log EC_{50} - [NrTP])}} \quad (3)$$

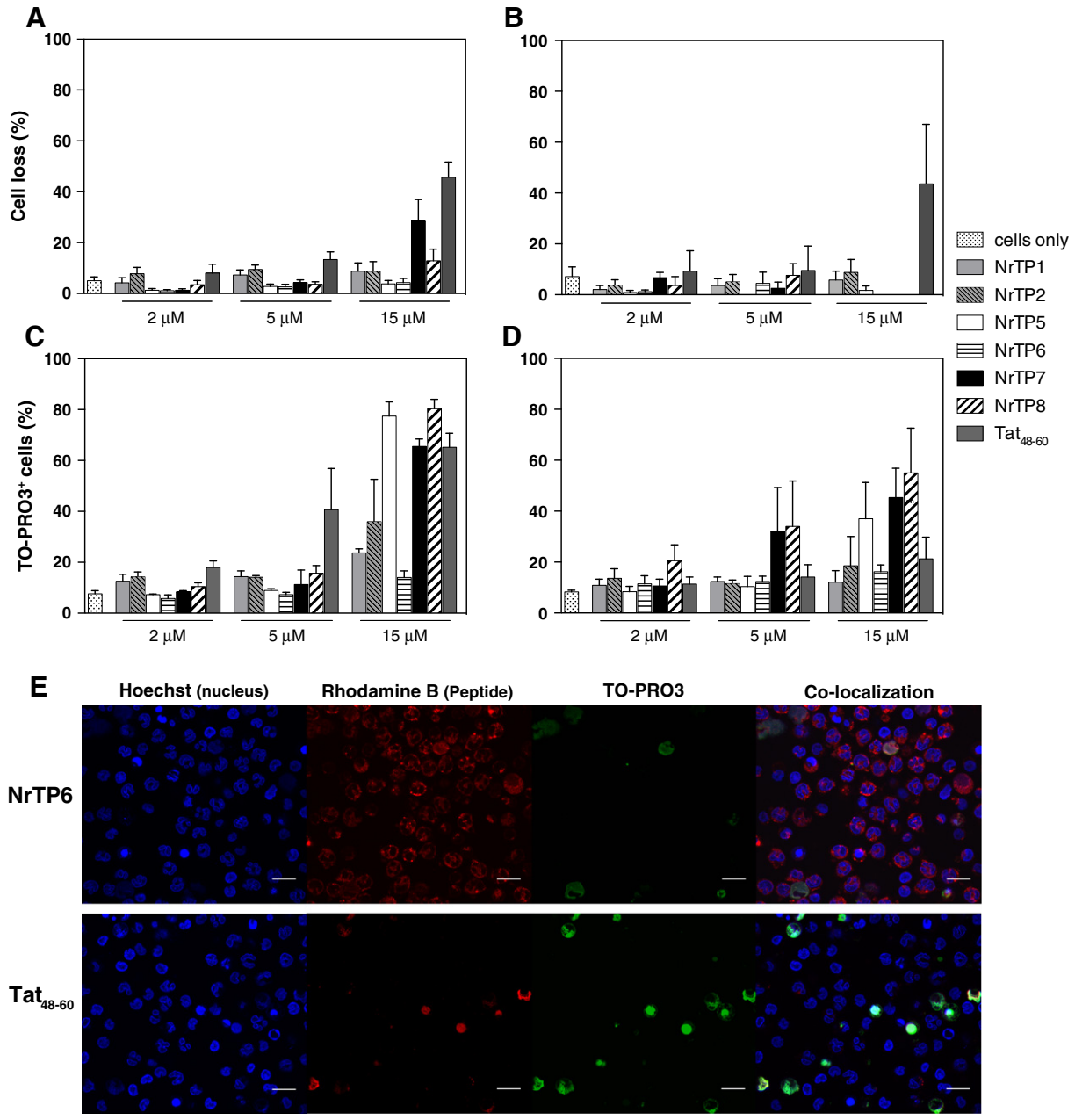

Fig. 5. Viability of PBMCs incubated with NrTPs. (A) Cell number variation after 2 h of incubation at 37 °C, for lymphocytes (A) and monocytes (B). TO-PRO3 viability analysis after the same treatments, for 2 h at 37 °C, for lymphocytes (C) and monocytes (D). Error bars represent SEM of 3 independent experiments. Statistical significance analysis (A–D) was conducted using two-way ANOVA and Dunnett's post-test (all peptides against unstained cells for each peptide concentration). For lymphocytes (A and C), there were statistically significant variations for specific peptide, their concentration and interaction (all with $p < 0.0001$). For monocytes, statistically significant variations were obtained for specific peptide ($p = 0.0053$) in (B), and both for specific peptide ($p = 0.0017$) and their concentration ($p = 0.0015$) in (D). Post-test significance results: (A) $p < 0.0001$ for 15 μM NrTP7 and $Tat_{48–60}$; (B) $p = 0.003$ for 15 μM $Tat_{48–60}$; (C) $p = 0.0001$ for 5 μM $Tat_{48–60}$, and at 15 μM $p = 0.0112$ for NrTP2 and $p < 0.0001$ for NrTP5, NrTP7, NrTP8 and $Tat_{48–60}$; (D) at 15 μM, $p = 0.0124$ for NrTP7 and $p = 0.001$ for NrTP8. Confocal microscopy images for NrTP6 or $Tat_{48–60}$ 15 μM after 2 h incubation at 37 °C (E). Scale bars = 15 μm.

where I_{max} and I_{min} are the maximum and minimum intensity of RhB fluorescence, respectively, EC_{50} is the peptide concentration at half way between I_{min} and I_{max}, [NrTP] is the peptide concentration and h is the Hill slope (already introduced in Eq. (1)) that here characterizes the curve steepness. This model describes standard dose response curves, for which h is a variable parameter ($h \neq 1$). I_{min} was fixed for each peptide as the average value obtained for 1 μM. Results from the fitting of Fig. 7 curves using Eq. (3) (Table 3) show $h > 1$ for all peptides, an indication of positive cooperativity in NrTP uptake. The cooperativity level is peptide-dependent and reasonably independent of cell type. NrTP7, both in lymphocytes and monocytes, shows higher cooperativity than other NrTPs, which may account for the presence of Arg instead of Lys residues and be related to its toxicity above 10 μM. As expected from the kinetic profiles, NrTP6 is the peptide reaching higher fluorescence values in lymphocytes, well above other NrTPs. On the other hand, in monocytes NrTP6 behaves very much like NrTP1, while NrTP7 is again the peptide with higher fluorescence, although cytotoxic.

4. Discussion

The methodology employed in this work is very suitable for studying peptide internalization, especially uptake by primary cells. PBMCs are suspension cells that need no special treatment (e.g., trypsinization) prior to cytometer measuring. Cytometric analysis is less time-

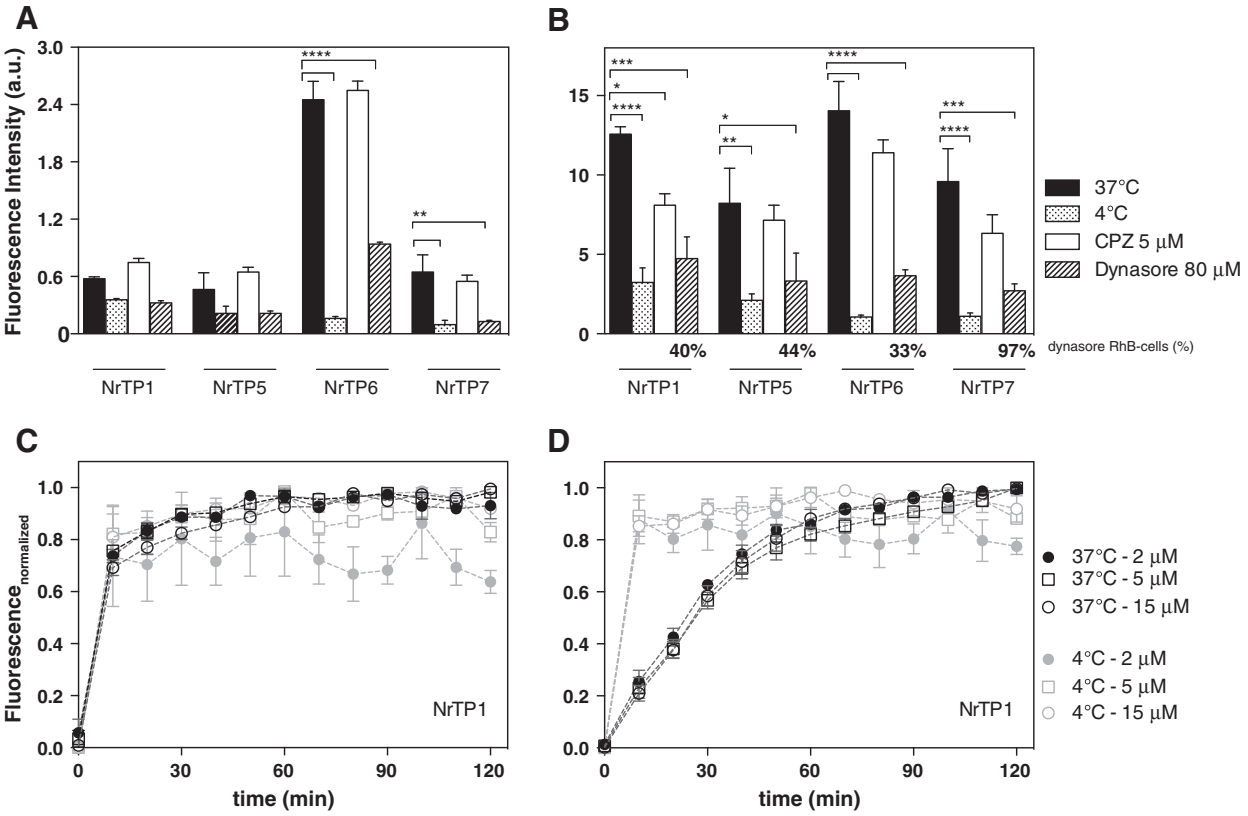

Fig. 6. NrTPs internalization at 4 °C and in the presence of endocytosis inhibitors, chlorpromazine and dynasore. Comparison between maximum values obtained for each peptide (5 µM) at 37 °C, 4 °C and in the presence of chemical inhibitors (at 37 °C), for lymphocytes (A) and monocytes (B). NrTP1 kinetic profiles, normalized for the maximum intensity, in lymphocytes (C) and monocytes (D), for 2, 5 and 15 µM at 4 °C and 37 °C. Error bars represent SEM of 3 independent experiments. Statistical significance analysis (A–B) was conducted using two-way ANOVA and Dunnett's post-test. Post-test comparisons were done for experiments at 4 °C and in the presence of endocytosis inhibitors against control experiments (37 °C without endocytosis inhibitors) for each peptide. For lymphocytes (A), statistically significant variations were associated to the specific peptide, treatment (4 °C or chemical inhibitors) and interaction ($p < 0.0001$), whereas for monocytes (B) significant variations were associated to the specific peptide ($p = 0.0069$) and treatment ($p < 0.0001$). Post-test significance represented in the figure corresponds to: *$p < 0.05$, **$p < 0.01$, ***$p < 0.001$, and ****$p < 0.0001$.

consuming than microscopy techniques, as different conditions can be tested in parallel, with better statistical significance due to the large number of cells analyzed. If necessary, the assay may be performed continuously, as long as physiologic conditions of temperature, homogeneity and oxygenation can be maintained, as it was the case here.

NrTP uptake by PBMCs was analyzed for two distinct cell populations, lymphocytes and monocytes, with major differences that reflect their distinct morpho-physiologies and roles in the immune system [17], but also the diversity of their membrane lipid, protein and glycan contents. NrTP uptake by PBMCs is concentration and time-dependent, with kinetics depending on peptide and cell type, but not on concentration.

Monocytes are much more auto-fluorescent than lymphocytes, which can explain the initial differences in fluorescence intensity. At any rate, time course profiles reveal that monocytes internalize 5, 10 or even 20 times more peptide than lymphocytes. Most likely, their propensity to capture debris [17] and the increased membrane permeability synergize with the main CPP entry mechanism (endocytosis or direct translocation), increasing peptide internalization. Cell size can also be a relevant factor: monocytes are larger and have lower

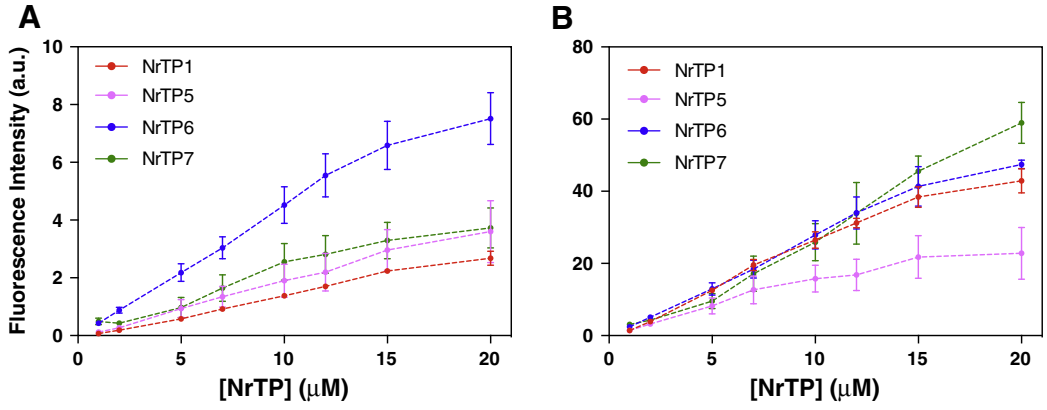

Fig. 7. Dose response curves for lymphocytes (A) and monocytes (B). NrTPs were tested from 1 to 20 µM. Error bars represent SEM of at least 3 independent experiments.

Table 3
Results obtained by the fitting of the dose response curves (using Eq. (3)): EC_{50} (peptide concentration for which fluorescence intensity is half way between the lowest and the highest value); h (Hill slope, steepness of the curve) and 95% CI (95% confidence interval for EC_{50}).

Peptide	Lymphocytes			Monocytes		
	EC_{50} (μM)	95% CI (μM)	h	EC_{50} (μM)	95% CI (μM)	h
NrTP1	15.2	10.7 to 21.4	1.8	10.8	8.2 to 14.1	1.8
NrTP5	20.2	8.2 to 49.9	1.5	9.2	5.5 to 15.3	1.7
NrTP6	10.8	8.2 to 14.3	1.9	11.9	9.5 to 14.9	1.9
NrTP7	9.2	8.1 to 10.4	2.9	17.2	13.0 to 22.9	2.1

nucleus-to-cytoplasm ratios than lymphocytes [17]. Significantly larger cytoplasm areas may also contribute to the higher fluorescence observed in monocytes.

NrTP uptake efficiencies on both PBMCs populations can be discussed on the basis of Figs. 3, 4 and 7, as well as Tables 2 and 3. In lymphocytes, differences between NrTP1 and NrTP6 regarding rate and total amount of internalized peptide are substantial, despite the minimal change in structure (Ser → Cys replacement in NrTP6). In monocytes, the opposite tendency (though to a smaller extent) prevails, and differences tend to narrow down with increasing peptide concentration. In terms of toxicity, NrTP6 performs consistently better than the rest. Interpreting the reduced toxicity and higher uptake of NrTP6 on the basis of the single Cys → Ser replacement might be simplistic, given that NrTP8, with identical sequence except for a rather conservative Trp → Tyr replacement, is internalized less efficiently and shows some toxicity. If anything, these results underscore the role of Ser and Tyr residues in NrTP6, the best performing CPP in the series (see below).

As previously mentioned, in lymphocytes the Tat_{48-60} < NrTP1 < NrTP5 < NrTP8 < NrTP2 < NrTP7 < NrTP6 ranking in peptide uptake is maintained for all three concentrations tested. However, in monocytes the ranking is different and shows some variation between concentrations (Fig. 3). For example, the low efficiency of NrTP7 at 2 μM improves significantly at higher concentrations, albeit with an increase in toxicity. Another contrast between both PBMCs populations is the effect of the 6-aminohexanoic acid spacer in NrTP2, which is irrelevant in lymphocytes while in monocytes it enhances uptake efficiency and slightly decreases toxicity relative to lymphocytes.

NrTP1 and NrTP5, its enantiomer, do not significantly differ in uptake kinetics in lymphocytes, although for NrTP5 a tendency to higher internalization is observed, as confirmed by the dose response curves (Fig. 7). In contrast, in monocytes, although both peptides (either at 2 or 5 μM) reach similar fluorescence values after 2 h incubation, the slower NrTP5 entry rate is maintained over time, leading to a higher NrTP5 intracellular concentration at equilibrium. For 15 μM, this difference is even more pronounced. The improved performance of the D-enantiomers of CPPs over their L-counterparts has been correlated with their higher resistance to proteolysis [21,24,36]. In the present case, as both NrTP1 and NrTP5 were efficiently internalized into PBMCs, internalization is not likely to be receptor-dependent, highlighting a significant role for direct translocation, as also found in our recent work with lipid model systems [14].

Most NrTPs in this study display, in both cell populations, approximately hyperbolic saturation curves within 2 h of experiment. However, initial rates in monocytes are slower than in lymphocytes, giving rise to sigmoidal-like profiles. Most probably, this difference is related to the entry mechanism and reflects a need for a given local peptide concentration to be attained before uptake by monocytes can take place, i.e., a cooperativity effect. Monocytes are phagocytic cells (a special form of endocytosis) that require signals to start internalizing external material. In our system, the signal is likely to be peptide accumulation on the cell membrane. A possible justification for differences in kinetics between PBMCs is that in lymphocytes direct translocation plays a more significant role than in monocytes. Direct translocation generally is a faster process than endocytosis, and that can explain the faster uptake kinetics (for most peptides) in lymphocytes, compared with monocytes. The only exceptions seem to be NrTP6 and NrTP7, where the higher uptake is probably due to a synergistic effect between both mechanisms. This effect can be easily explained for NrTP7, an Arg containing-peptide that, as previously shown, can use both direct translocation and endocytosis as internalization mechanisms [9,36,37].

Endocytosis was previously shown to be a predominant mechanism of NrTP entry into cancer cells [16]. The present results for peptide uptake at 4 °C, especially for lymphocytes, hint at an important role for direct translocation, as already observed in biomembrane model systems [14]. In these systems, both NrTP1 and NrTP5 were seen to translocate lipid vesicles in the absence of receptors or transmembrane potentials, therefore excluding endocytosis as the sole entry mechanism. However, it is worth to notice that, in monocytes, the substantial differences in entry rates between 4 °C and 37 °C (Fig. 6B) suggest a main role for endocytosis under physiologic conditions.

Viability assays on cells retaining the native scattering properties (i.e., still within the original flow cytometry gates; Figs. 5, S3, S4, S5 and S10) show that most NrTPs are non-toxic for PBMCs within the range of concentrations tested. The combined interpretation of three different viability assays (cell number loss, TO-PRO3 and annexin V) allows us to conclude that Tat_{48-60} and NrTP7 are the only ones causing cell membrane disruption, in agreement with the observation that Arg-containing peptides are typically more toxic than Lys-containing ones [38].

NrTP5 and NrTP8, though not inducing cell loss, caused the presence of TO-PRO3 labeled cells (≥15 μM), mostly in lymphocytes (Fig. 5A–B, S3). For NrTP5, decreased susceptibility to proteolysis may explain this result. Alternatively, it may simply be due to membrane alterations as consequence of its entry mechanism(s), enabling TO-PRO3 entry without effective cell death. Of all CPPs of this study, NrTP1 and NrTP6 are strictly non-toxic, with NrTP6 clearly as the best overall performer of this new CPP family. In fact, NrTP6 can even be associated to some sort of "cell protection", as variation in cell number was lower than for control cells and TO-PRO3 fluorescence intensity in monocytes also presented lower values.

It is worth noting that NrTPs display higher uptake efficiency and lower toxicity than Tat_{48-60}, a paradigm in CPP studies [39]. While most literature on CPP internalization describes experiments in cancer cell lines (easier to transfect than healthy primary cells), in the present work we assessed the potential of NrTPs as delivery agents for pathologies associated with human primary immune cells. For example, the elevated regulatory T cell (T_{reg}) levels found in cancer patients [40], impairing anti-tumor and anti-viral immunity, could be decreased by NrTP6-mediated delivery of molecules that specifically interfere with T_{reg} critical mechanisms [41]. siRNA technology has been used in combination with CPPs with promising results [42]. In this regard, NrTPs could also be used in HIV-1 infected patients for targeting $CD4^+$ T-cells, the major subgroup of T cells [43] and the main target for HIV infection. When $CD4^+$ counts decrease below a critical level, cell-mediated immunity is lost, and the body becomes progressively more susceptible to opportunistic infections [44]. A possible therapeutic strategy is to impair the activity of Rev, a protein responsible for inhibiting viral RNA splicing [45]. Thus, a conjugate of NrTP6 and siRNA coding for Rev might significantly decrease HIV-1 infection by silencing Rev expression. This is a simpler approach than that described by Roisin et al. [46], where several constructs of small proteins containing Rev elements were produced and transfected onto cells. These therapeutic applications combine the use of immune cells (such as PBMCs) with the particular intracellular localization of NrTPs (cytosol). The cytoplasm is a well-known venue for diverse biological processes involved in disease. Thus, it is not surprising that cytosolic delivery is considered as a desirable sub-cellular target for therapeutic

molecules such as anticancer drugs and siRNAs [47]. Upon conjugation with CPPs, these molecules may easily gain cellular access to accomplish their specific tasks [47–49].

In conclusion, the present work stresses the potential of NrTPs as translocation tools. Uptake kinetic data and viability tests point to NrTP6 as a preferred NrTP, with high efficiency and no cell toxicity, in PBMCs. Our study also reinforces flow cytometry as a particularly appropriate methodology to monitor CPP entry into primary cells or other cells in suspension.

Supplementary data to this article can be found online at http://dx.doi.org/10.1016/j.bbagen.2013.05.020.

Acknowledgements

The authors thank Teresa Freitas (IMM) for PBMCs isolation and to Telma Lança (IMM) for valuable discussions. This work was funded by Fundação para a Ciência e a Tecnologia — Ministério da Educação e Ciência (FCT-MEC, Portugal), including M.R. PhD fellowship SFRH/BD/37432/2007, Spanish Ministry of Economy and Competitiveness (MINECO, grant SAF2011-24899), Generalitat de Catalunya (2009 SGR 492) and FP7-PEOPLE IRSES project MEMPEPACROSS (European Union).

References

[1] K.M. Stewart, K.L. Horton, S.O. Kelley, Cell-penetrating peptides as delivery vehicles for biology and medicine, Org. Biomol. Chem. 6 (2008) 2242–2255.
[2] E. Koren, V.P. Torchilin, Cell-penetrating peptides: breaking through to the other side, Trends Mol. Med. 18 (2012) 385–393.
[3] J.R. Luque-Ortega, B.G. de la Torre, V. Hornillos, J.-M. Bart, C. Rueda, M. Navarro, F. Amat-Guerri, A.U. Acuña, D. Andreu, L. Rivas, Defeating Leishmania resistance to Miltefosine (hexadecylphosphocholine) by peptide-mediated drug smuggling: a proof of mechanism for trypanosomatid chemotherapy, J. Control. Release 161 (2012) 835–842.
[4] J.B. Rothbard, S. Garlington, Q. Lin, T. Kirschberg, E. Kreider, P.L. McGrane, P.A. Wender, P.A. Khavari, Conjugation of arginine oligomers to cyclosporin A facilitates topical delivery and inhibition of inflammation, Nat. Med. 6 (2000) 1253–1257.
[5] B. Lebleu, H.M. Moulton, R. Abes, G.D. Ivanova, S. Abes, D.A. Stein, P.L. Iversen, A.A. Arzumanov, M.J. Gait, Cell penetrating peptide conjugates of steric block oligonucleotides, Adv. Drug Deliv. Rev. 60 (2008) 517–529.
[6] F. Meyer-Losic, C. Nicolazzi, J. Quinonero, F. Ribes, M. Michel, V. Dubois, C. De Coupade, M. Boukaissi, A.-S. Chéné, I. Tranchant, V. Arranz, I. Zoubaa, J.-S. Fruchart, D. Ravel, J. Kearsey, DTS-108, a novel peptidic prodrug of SN38: in vivo efficacy and toxicokinetic studies, Clin. Cancer Res. 14 (2008) 2145–2153.
[7] V. Sebbage, Cell-penetrating peptides and their therapeutic applications, Biosci. Horiz. 2 (2009) 64–72.
[8] R.M. Johnson, S.D. Harrison, D. Maclean, Therapeutic applications of cell-penetrating peptides, Methods Mol. Biol. 683 (2011) 535–551.
[9] F. Madani, S. Lindberg, U. Langel, S. Futaki, A. Gräslund, Mechanisms of cellular uptake of cell-penetrating peptides, J. Biophys. 2011 (2011) 414729.
[10] G. Ter-Avetisyan, G. Tünnemann, D. Nowak, M. Nitschke, A. Herrmann, M. Drab, M.C. Cardoso, Cell entry of arginine-rich peptides is independent of endocytosis, J. Biol. Chem. 284 (2009) 3370–3378.
[11] J.R. Maiolo, M. Ferrer, E.A. Ottinger, Effects of cargo molecules on the cellular uptake of arginine-rich cell-penetrating peptides, Biochim. Biophys. Acta 1712 (2005) 161–172.
[12] G. Tünnemann, R.M. Martin, S. Haupt, C. Patsch, F. Edenhofer, M.C. Cardoso, Cargo-dependent mode of uptake and bioavailability of TAT-containing proteins and peptides in living cells, FASEB J. 20 (2006) 1775–1784.
[13] G. Rádis-Baptista, B.G. de la Torre, D. Andreu, A novel cell-penetrating peptide sequence derived by structural minimization of a snake toxin exhibits preferential nucleolar localization, J. Med. Chem. 51 (2008) 7041–7044.
[14] M. Rodrigues, A. Santos, B.G. de la Torre, G. Rádis-Baptista, D. Andreu, N.C. Santos, Molecular characterization of the interaction of crotamine-derived nucleolar targeting peptides with lipid membranes, Biochim. Biophys. Acta 1818 (2012) 2707–2717.
[15] M. Rodrigues, B.G. de la Torre, G. Rádis-Baptista, N.C. Santos, D. Andreu, Efficient cellular delivery of β-galactosidase mediated by NrTPs, a new family of cell-penetrating peptides, Bioconjug. Chem. 22 (2011) 2339–2344.
[16] G. Rádis-Baptista, B.G. de la Torre, D. Andreu, Insights into the uptake mechanism of NrTP, a cell-penetrating peptide preferentially targeting the nucleolus of tumour cells, Chem. Biol. Drug Des. 79 (2012) 907–915.
[17] A.K. Abbas, A.H.H. Lichtman, S. Pillai, Cellular and Molecular Immunology, Saunders, 2011.
[18] M. Tavecchio, M. Simone, S. Bernasconi, G. Tognon, G. Mazzini, E. Erba, Multiparametric flow cytometric cell cycle analysis using TO-PRO-3 iodide (TP3): detailed protocols, Acta Histochem. 110 (2008) 232–244.
[19] N. Marina-Garcia, L. Franchi, Y.G. Kim, Y. Hu, D.E. Smith, G.J. Boons, G. Nuñez, Clathrin- and dynamin-dependent endocytic pathway regulates muramyl dipeptide internalization and NOD2 activation, J. Immunol. 182 (2009) 4321–4327.
[20] E. Macia, M. Ehrlich, R. Massol, E. Boucrot, C. Brunner, T. Kirchhausen, Dynasore, a cell-permeable inhibitor of dynamin, Dev. Cell 10 (2006) 839–850.
[21] P.A. Wender, D.J. Mitchell, K. Pattabiraman, E.T. Pelkey, L. Steinman, J.B. Rothbard, The design, synthesis, and evaluation of molecules that enable or enhance cellular uptake: peptoid molecular transporters, Proc. Natl. Acad. Sci. U. S. A. 97 (2000) 13003–13008.
[22] A. Manceur, A. Wu, J. Audet, Flow cytometric screening of cell-penetrating peptides for their uptake into embryonic and adult stem cells, Anal. Biochem. 364 (2007) 51–59.
[23] L. Cascales, S.T. Henriques, M.C. Kerr, Y.-H. Huang, M.J. Sweet, N.L. Daly, D.J. Craik, Identification and characterization of a new family of cell-penetrating peptides: cyclic cell-penetrating peptides, J. Biol. Chem. 286 (2011) 36932–36943.
[24] S. Jones, J. Howl, Enantiomer-specific bioactivities of peptidomimetic analogues of mastoparan and mitoparan: characterization of inverso mastoparan as a highly efficient cell penetrating peptide, Bioconjug. Chem. 23 (2012) 47–56.
[25] I. Schmid, M.A. Hausner, S.W. Cole, C.H. Uittenbogaart, J.V. Giorgi, B.D. Jamieson, Simultaneous flow cytometric measurement of viability and lymphocyte subset proliferation, J. Immunol. Methods 247 (2001) 175–186.
[26] H. Hirose, T. Takeuchi, H. Osakada, S. Pujals, S. Katayama, I. Nakase, S. Kobayashi, T. Haraguchi, S. Futaki, Transient focal membrane deformation induced by arginine-rich peptides leads to their direct penetration into cells, Mol. Ther. 20 (2012) 984–993.
[27] C. Palm-Apergi, P. Lönn, S.F. Dowdy, Do cell-penetrating peptides actually "penetrate" cellular membranes? Mol. Ther. 20 (2012) 695–697.
[28] G. Kroemer, L. Galluzzi, P. Vandenabeele, J. Abrams, E.S. Alnemri, E.H. Baehrecke, M.V. Blagosklonny, W.S. El-Deiry, P. Golstein, D.R. Green, M. Hengartner, R.A. Knight, S. Kumar, S.A. Lipton, W. Malorni, G. Nuñez, M.E. Peter, J. Tschopp, J. Yuan, M. Piacentini, et al., Classification of cell death: recommendations of the Nomenclature Committee on Cell Death 2009, Cell Death Differ. 16 (2009) 3–11.
[29] A.I. Ivanov, Pharmacological inhibition of endocytic pathways: is it specific enough to be useful? Methods Mol. Biol. 440 (2008) 15–33.
[30] D. Vercauteren, R.E. Vandenbroucke, A.T. Jones, J. Rejman, J. Demeester, S.C. De Smedt, N.N. Sanders, K. Braeckmans, The use of inhibitors to study endocytic pathways of gene carriers: optimization and pitfalls, Mol. Ther. 18 (2010) 561–569.
[31] T. Kirchhausen, E. Macia, H.E. Pelish, Use of dynasore, the small molecule inhibitor of dynamin, in the regulation of endocytosis, Methods Enzymol. 438 (2008) 77–93.
[32] G.J. Doherty, H.T. McMahon, Mechanisms of endocytosis, Annu. Rev. Biochem. 78 (2009) 857–902.
[33] I. Kocić, J. Ruczyński, R. Szczepańska, M. Olkowicz, B. Parfianowicz, I. Rusiecka, P. Rekowski, Cell-penetrating peptides modulate the vascular action of phenylephrine, Pharmacol. Rep. 63 (2011) 195–199.
[34] S.J. Edelstein, N. Le Novère, Cooperativity of allosteric receptors, J. Mol. Biol. 425 (2013) 1424–1432.
[35] N. Bindslev, Hill in hell, Modeling Theoretical Tools to Test and Evaluate Experimental Equilibrium Effects, Co-Action Publishing, 2008, pp. 257–282.
[36] G. Tünnemann, G. Ter-Avetisyan, R.M. Martin, M. Stöckl, A. Herrmann, M.C. Cardoso, Live-cell analysis of cell penetration ability and toxicity of oligo-arginines, J. Pept. Sci. 14 (2008) 469–476.
[37] H.A. Rydberg, M. Matson, H.L. Åmand, E.K. Esbjörner, B. Nordén, Effects of tryptophan content and backbone spacing on the uptake efficiency of cell-penetrating peptides, Biochemistry 51 (2012) 5531–5539.
[38] D.J. Mitchell, D.T. Kim, L. Steinman, C.G. Fathman, J.B. Rothbard, Polyarginine enters cells more efficiently than other polycationic homopolymers, J. Pept. Res. 56 (2000) 318–325.
[39] J.S. Wadia, S.F. Dowdy, Transmembrane delivery of protein and peptide drugs by TAT-mediated transduction in the treatment of cancer, Adv. Drug Deliv. Rev. 57 (2005) 579–596.
[40] M. Beyer, J.L. Schultze, Regulatory T cells in cancer, Blood 108 (2006) 804–811.
[41] M.A. Morse, A. Hobeika, D. Serra, K. Aird, M. Mckinney, A. Aldrich, T. Clay, D. Mourich, H.K. Lyerly, P.L. Iversen, G.R. Devi, Depleting regulatory T cells with arginine-rich, cell-penetrating, peptide-conjugated morpholino oligomer targeting FOXP3 inhibits regulatory T-cell function, Cancer Gene Ther. 19 (2012) 30–37.
[42] S.E.L. Andaloussi, T. Lehto, I. Mäger, K. Rosenthal-Aizman, I.I. Oprea, O.E. Simonson, H. Sork, K. Ezzat, D.M. Copolovici, K. Kurrikoff, J.R. Viola, E.M. Zaghloul, R. Sillard, H.J. Johansson, F. Said Hassane, P. Guterstam, J. Suhorutšenko, P.M.D. Moreno, N. Oskolkov, J. Hälldin, et al., Design of a peptide-based vector, PepFect6, for efficient delivery of siRNA in cell culture and systemically in vivo, Nucleic Acids Res. 39 (2011) 3972–3987.
[43] M. Pope, A.T. Haase, Transmission, acute HIV-1 infection and the quest for strategies to prevent infection, Nat. Med. 9 (2003) 847–852.
[44] R.A. Weiss, How does HIV cause AIDS? Science 260 (1993) 1273–1279.
[45] W.C. Greene, B.M. Peterlin, Charting HIV's remarkable voyage through the cell: basic science as a passport to future therapy, Nat. Med. 8 (2002) 673–680.
[46] A. Roisin, J.-P. Robin, N. Dereuddre-Bosquet, A.-L. Vitte, D. Dormont, P. Clayette, P. Jalinot, Inhibition of HIV-1 replication by cell-penetrating peptides binding Rev, J. Biol. Chem. 279 (2004) 9208–9214.
[47] L. Rajendran, H.-J. Knölker, K. Simons, Subcellular targeting strategies for drug design and delivery, Nat. Rev. Drug Discov. 9 (2010) 29–42.
[48] A. Eguchi, B.R. Meade, Y.-C. Chang, C.T. Fredrickson, K. Willert, N. Puri, S.F. Dowdy, Efficient siRNA delivery into primary cells by a peptide transduction domain–dsRNA binding domain fusion protein, Nat. Biotech. 27 (2009) 567–571.
[49] S. Veldhoen, S.D. Laufer, T. Restle, Recent developments in peptide-based nucleic acid delivery, Int. J. Mol. Sci. 9 (2008) 1276–1320.